SEMARAK ILMU PUBLISHING

Journal of Advanced Research in Micro and Nano Engineering

Journal homepage:
https://semarakilmu.com.my/journals/index.php/micro_nano_engineering/index
ISSN: 2756-8210

Effect of PANI-Doped-Graphene Oxide as HTL in Perovskite Solar Cells Using SCAPS-1D Software

Nabilah Ahmad Jalaludin[1], Fauziyah Salehuddin[1,*], Faiz Arith[1], Khairil Ezwan Kaharudin[2], Anis Suhaila Mohd Zain[1], Ibrahim Ahmad[3], Siti Aisah Mat Junos[1], Prakash R Apte[4]

[1] Micro & Nano Electronics (MiNE), CeTRI, Faculty of Electronics & Computer Technology and Engineering (FTKEK), Universiti Teknikal Malaysia Melaka, Hang Tuah Jaya, Durian Tunggal, 76100 Melaka, Malaysia
[2] Faculty of Engineering, Lincoln University College (Main Campus), Wisma Lincoln, 47301 Petaling Jaya, Selangor, Malaysia
[3] College of Engineering (CoE), Universiti Tenaga Nasional (UNITEN), 43009 Kajang, Selangor, Malaysia
[4] Indian Institute of Technology (IIT), Bombay, Powai, Mumbai 400076, India

ARTICLE INFO

Article history:
Received 8 August 2024
Received in revised form 19 September 2024
Accepted 29 October 2024
Available online 30 November 2024

Keywords:
SCAPS-1D; PSC; PANI; graphene oxide; hole transport layer

ABSTRACT

This research examines and analyses the solar cell performance of methylammonium lead triiodide ($MAPbI_3$) perovskite solar cells (PSC) that utilize Polyaniline (PANI)-doped-graphene oxide (GO) as HTL. Additionally, the study used the SCAPS-1D simulation software to model and analyze the experimental data. The simulated data generated by the SCAPS-1D software is afterward compared to the experimental findings. This comparison serves as a foundation for further optimization of the solar cell's performance. This study explicitly examined the impact of layer thickness and doping density on device performance in order to determine which parameters should be optimized to enhance overall performance. The SCAPS-1D simulation obtained a highest power conversion efficiency (PCE) of 15.37%. This work presented an improved efficiency of 40% from the experimental data. The findings of our study have the potential to be used in the prediction of key parameters for the optimization of perovskite solar cells (PSCs) using doped PANI/GO as a hole transport layer (HTL).

1. Introduction

Graphene has garnered significant technical interest, particularly within the realm of nanotechnology, since 2004 [1,2]. A graphene sheet is a single layer of atoms organized in a hexagonal configuration, bound together by covalent bonds, resulting in exceptional mechanical strength [3,4]. After extensive investigation and scholarly inquiry spanning ten years, graphene has been substantiated as exhibiting a notable level of carrier mobility (specifically, 2 × 105 cm^2/Vs for suspended graphene) when subjected to ambient temperatures. Additionally, it has been observed to possess exceptional transparency, with a light absorption rate of approximately 2.3% across a wide range of ultraviolet (UV) and visible wavelengths. Furthermore, graphene has been found to possess a high degree of thermal conductivity, and an elevated melting point of approximately 5000 K [5]. In

* *Corresponding author.*
E-mail address: fauziyah@utem.edu.my

https://doi.org/10.37934/armne.25.1.3951

addition to this, the atom-layer arrangement of graphene sheets may also derive advantages from their substantial surface area and notable flexibility. The low-cost graphene technology is considered well-suited for various applications, including photovoltaic cells, chemical sensors, medical devices, photo-detectors [6-8], energy storage, and manufacturing roll-to-roll electronic devices.

Graphene can potentially enhance charge injection and collection at the electrodes, resulting in increased power conversion efficiency and durability. Various methodologies were used to create a novel composite material known as HTL. The perovskite film deposited on graphene oxide (GO) exhibited superior film coverage and bigger crystal size compared to conventional poly(3,4-ethylenedioxythiophene): poly(styrenesulfonate) (PEDOT:PSS) and indium tin oxide (ITO) without any further treatment. Moreover, the use of perovskite on a graphene oxide (GO) layer has been shown to exhibit a significant enhancement in carrier mobility inside the conducting channel, thus leading to improved carrier separation and Jsc. The use of a PSC device with a graphene oxide (GO) layer as the hole transport layer (HTL) resulted in a notable enhancement of the power conversion efficiency (PCE) by about 25.3% in comparison to the device using PEDOT:PSS [9].

Additionally, the use of a graphene oxide (GO) layer with a greater density of acceptor sites and increased thickness may provide improved enhancements when combined with perovskite, thus leading to an increase in the power conversion efficiency (PCE). A comparative analysis was conducted between a recent study using reduced graphene oxide (r-GO) as a hole transport layer (HTL) and the conventional spiro-OMeTAD material. The transfer characteristics of perovskite solar cells (PSCs) indicate that Spiro-OMeTAD exhibits a higher power conversion efficiency (PCE) primarily as a result of the presence of both types of graphene oxide (GO) layers. Moreover, no statistical disparity is seen in the device efficiency between spin-coated and sprayed GO-based PSCs. Nevertheless, the efficiency of perovskite solar cells (PSCs), including Spiro-OMeTAD, saw a significant decline of 41% after a duration of 1987 hours, mainly attributed to the poor stability of Spiro-OMeTAD. Meanwhile, it was shown that perovskite solar cells (PSCs), including graphene oxide (GO), exhibited notable stability and a noteworthy enhancement in power conversion efficiency (PCE). Specifically, the PCE improved from 4.87% to 6.62%, representing a 36% gain in efficiency. This improvement may be attributed to the superior suppression of photo-generated carrier recombination at the GO layer compared to Spiro-OMeTAD, as reported by Palma *et al.,* [10].

Apart from being applied for HTL, graphene may also be utilized as the contact electrode in perovskite solar cells (PSC) owing to its tunable conductivity, high carrier mobility, and transparency. Photovoltaic solar cells (PSCs) that are in touch with a graphene electrode have the potential to receive light from both sides. According to a recent study conducted by You *et al.,* [11], the transfer of chemically vapor deposition (CVD)-synthesized graphene was facilitated by using a layer of polymethyl methacrylate (PMMA) on top of a thin film of poly(3,4-ethylenedioxythiophene):poly(styrenesulfonate) (PEDOT:PSS). This approach was shown to be effective in modulating the conductivity of the graphene electrodes. The photovoltaic cells (PSCs) in question, including two-layer graphene electrodes, have a power conversion efficiency (PCE) of 12.02% when illuminated from the FTO side and 11.65% when illuminated from the graphene side. A recent study done by Kang *et al.,* [12] investigated a graphene-contacting perovskite solar cell (PSC) configuration, where reduced graphene oxide (r-GO) was deposited on the top electrode and also served as the hole transport layer (HTL). The results suggest that graphene has the potential to serve as a viable alternative to traditional Spiro-MeOTAD-based perovskite solar cells (PSCs), although exhibiting a slightly reduced fill factor.

Polyaniline (PANI) is considered a promising option for photovoltaic devices due to its desirable characteristics, including high conductivity, environmental stability, affordability, ease of synthesis, high purity, transparency in thin films, and excellent processability [13]. These features make

polyaniline well-suited for application in perovskite solar cells. In previous work reported by Habib *et al.,* [14], they achieved a PCE of 9.24% utilising doped PANI/GO as HTL. This modified cell exhibits enhanced efficiency compared to the pristine GO PSC. In a separate study conducted by Mabrouk *et al.,* [15], a notable advancement was achieved in the performance of inverted PSCs. Using a mixed dopant of graphene oxide (GO) and polyaniline (PANI), the researchers attained a significantly enhanced efficiency of 18.12%. Moreover, this modified cell exhibited superior stability to the conventional PEDOT:PSS cell.

The use of device simulations proves advantageous in the examination of different characteristics associated with each perovskite solar cell (PSC) layer. This practice serves as a preliminary guide prior to the fabrication procedure, aiming to enhance the performance of cell efficiency and minimize the expenses incurred during fabrication. In this study, a numerical analysis has been conducted to evaluate and examine many important parameters, including V_{OC}, J_{SC}, FF, and PCE.

This work study the performance of each layer, including the electron transport layer (ETL), absorber layer, and hole transport layer (HTL). These layers are optimized by the examination of many factors, including thickness and doping density. The numerical study was conducted using a SCAPS-1D software operating under AM1.5G illumination conditions.

2. Methodology

This section explains and provides the implementation method and data gathered using simulation to obtain and attain the required project objectives. SCAPS-1D simulation software is employed to design and simulate the devices by using a lead-based absorber layer, $MAPbI_3$, doped PANI/GO as HTL and PCBM as ETL. SCAPS-1D used in this study for studies the effect of HTL, ETL and absorber layer thickness, and doping density on the main electrical parameters of the PSC. The performance is analysed through the J-V characteristics that have been obtained.

2.1 Device Simulation

SCAPS-1D is a solar cell modelling or simulation program created at Gent University. The program has the capability to replicate the operational characteristics of multilayer solar cells [16,17]. The solar cell parameters can be attained by solving the fundamental equations that describe the charge transport in semiconductors, which are presented below [18]. Poisson equation:

$$\frac{dE}{dx} = -\frac{d^2\Psi}{dx^2} = \frac{q}{\varepsilon}\left[p(x) - n(x) + N_D^+(x) - N_D^-(x) + \rho_t(x) - n_t(x)\right] \quad (1)$$

where E is the electric field, q is the electron charge, Ψ is the electrostatic potential, ε is the dielectric constant of the semiconductor material, $p(n)$ is the hole (electron) concentration, $N_D^-(N_D^+)$ is the density of the ionized acceptors (donors), n_t (p_t) is the trapped electron (hole), and x is the position coordinate. The following are the continuity equations for holes Eq. (2) and Eq. (3) electrons [18]:

$$\frac{dp_n}{dt} = G_n - \frac{p_n - p_{n0}}{\tau_p} + p_n\mu_p\frac{dE}{dx} + \mu_n E\frac{dp_n}{dx} + D_p\frac{d^2p_n}{dx^2} \quad (2)$$

$$\frac{dn_p}{dt} = G_n - \frac{n_p - n_{p0}}{\tau_n} + n_p\mu_n\frac{dE}{dx} + \mu_n E\frac{dn_p}{dx} + D_n\frac{d^2n_p}{dx^2} \quad (3)$$

where G_n represents electron generation rates, G_p represents hole generation rates, D_n represents electron diffusion coefficients, and D_p represents hole diffusion coefficients.

In this study, the simulation was first conducted in line with the device design, as reported by Habib *et al.,* [14]. The PSC simulation consists of five layers: FTO, ETL (PCBM), absorber layer ($MaPbI_3$), HTL (doped PANI/GO), and back contact (Ag), as shown in Figure 1. However, in this study, the solar cell structure was simulated in conventional structure compared to the experimental paper (inverted structure of PSC). The performance of PSC is analysed based on the value parameter of the resulting efficiency (PCE%) with different layer thicknesses and doping densities. The numerical study was conducted using a SCAPS-1D software operating under AM1.5G illumination conditions. The overall SCAPS input and basic parameters of each material are referred to in the previous works, as displayed in Tables 1, 2, and 3.

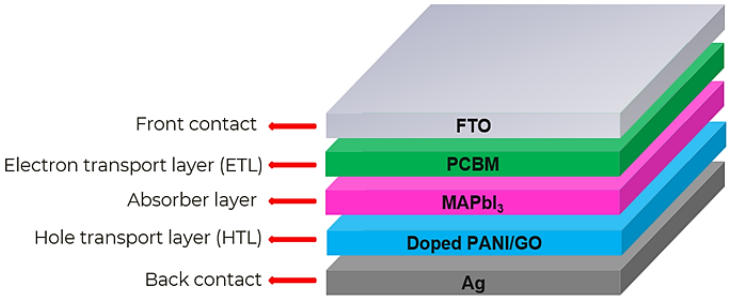

Fig. 1. The structure of PSC

Table 1
Input parameters of the component in device modelling of PSC

Parameters	PCBM [19]	$MAPbI_3$ [20]	Doped PANI/GO [20,21]
Layer thickness, d (nm)	10 (varies)	1500 (varies)	500 (varies)
Bandgap energy, E_g (eV)	2.1	1.58	2.76 [12]
Electron affinity, (eV)	3.9	3.9	2.02
Dielectric permittivity, ε (relative)	3.9	10	10
Conduction band density of states, N_C (cm^{-3})	2.2×10^{19}	2.2×10^{18}	2.2×10^{18}
Valence band density of states, N_V (cm^{-3})	2.2×10^{19}	1.0×10^{19}	1.8×10^{19}
Electron thermal velocity, V_c (cm/s)	1.0×10^{7}	1.0×10^{7}	1.0×10^{7}
Hole thermal velocity, V_h (cm/s)	1.0×10^{7}	1.0×10^{7}	1.0×10^{7}
Electron mobility, μ_e (cm^2/Vs)	0.001	2.2	26 [18]
Hole mobility, μ_p (cm^2/Vs)	0.002	2.2	36.2 [12]
Density of donor, N_D (cm^{-3})	1.0×10^{18}	NA	NA
Density of acceptor, N_A (cm^{-3})	NA	1.0×10^{17}	2.0×10^{17}

Table 2
Input parameters of the interface layer of PSC

Parameters	GO/$MAPbI_3$	$MAPbI_3$/PCBM
Defect type	Neutral	Neutral
Capture cross section electrons (cm^2)	1.0×10^{-19}	1.0×10^{-15}
Capture cross section holes (cm^2)	1.0×10^{-19}	1.0×10^{-15}
Energetic distribution	Single	Single
Reference for defect energy level (E_t)	Above the highest E_V	Above the highest E_V
Energy with respect to reference (eV)	0.60	0.60
Total density (integrated over all energies) (cm^{-2})	1.0×10^{10}	1.0×10^{12}

Table 3
Input parameters of front and back contact

Parameters	FTO [22]	Ag [23]
Surface recombination velocity of electrons (cm/s)	1.0×10^{7}	1.0×10^{5}
Surface recombination velocity of holes (cm/s)	1.0×10^{5}	1.0×10^{7}
Metal work function (Ev)	4.4	4.74

3. Results

This section will discuss the result obtained and the theory related to the work study that had been performed successfully. Different parameters are observed and measured to obtain better performance and best cell efficiency. Initially, the comparison of initial simulation and experimental has been committed to demonstrate the effectiveness of our simulation study. Next, the crucial process, which is to obtain an optimum parameter for the PSC component, has been carried out. In this study, the open-circuit voltage (V_{OC}), short-circuit current density (J_{SC}), fill factor (FF) and power conversion efficiency (PCE) of the solar cell were considered to be recorded and analysed from the J-V curve obtained. The optimum value of the parameter obtained was used for the following process to find the maximum efficiency of doped PANI/GO-based PSC with the influence of Ag as a back contact.

3.1 The Comparison of Initial Simulation and Experimental

The findings have been compared to the experimental findings presented by Habib *et al.,* [14] allowing us to illustrate the efficacy of our simulation study. Table 4 presents a comparative analysis highlighting the outcomes obtained from simulation and experimental data. The modelling study was carried out utilizing the first parameters outlined in Tables 1, 2, and 3. The outcome of the analysis demonstrated the performance of the perovskite solar cells (PSCs) with a short-circuit current density (J_{SC}) of 21.4025 mA/cm^2, an open-circuit voltage (V_{OC}) of 0.6377 V, a fill factor (FF) of 66.26%, and a power conversion efficiency (PCE) of 9.04%. The findings exhibit a strong correspondence, indicating the successful validation of our simulation. The findings of this study indicate that there is no statistically significant difference between the simulated and experimental values.

Table 4
Comparison of initial simulation and experimental

Solar Cell	Method	V_{OC} (V)	J_{SC} (mA/cm^2)	FF (%)	PCE (%)	Ref.
Inverted PSC	Experimental	0.52	21.23	67	9.24	[14]
Conventional PSC	Simulation	0.6377	21.4025	66.26	9.04	This work

3.2 Effect of PCBM Thickness and Doping Donor Density

The ETL, or electron transport layer, plays a vital role in the process of charge movement and collection inside the PSC. Additionally, it effectively inhibits the recombination of electrons and holes at the interface [24]. Hence, this research endeavour examined several characteristics associated with the ETL that have an impact on the efficiency of PSCs (Perovskite Solar Cells). These parameters included ETL thickness and doping density.

The effect of thickness is measured by varying the layer thickness of PCBM from a range of 10 nm to 100 nm. Figure 2 illustrates the graph analysis based on the different layer thickness of PCBM. According to the data shown in Figure 2, the simulation results indicate a reduction in the V_{OC} and

J_{SC}, while the fill factor shows an increase, when the thickness of the PCBM layer increases from 10 nm to 100 nm. Next, based on graph PCE, it shows that the increase in the layer thickness of PCBM resulted in decreases in efficiency. This is because a thick ETL might have a variety of effects. For instance, electron transport is limited to FTO. Second, it boosts the rate of recombination, which lowers the open-circuit voltage. Third, it increases the series resistance of the device, which reduces the fill factor and the efficiency of the solar cells. Electrons must travel a greater distance to reach the top electrode, FTO, as the thickness of the layer increases. Because of the long path length, electrons are more likely to recombine with minority carriers (holes). As a result, the drop in solar cell efficiency is mainly attributable to a decrease in fill factor resulting from increasing series resistance [25].

In this study, the doping donor density (N_D) value varied from 10^{15} cm^{-3} to 10^{20} cm^{-3}. The graph displays that V_{OC} and J_{SC} have a similar trend in which the value decreases at a certain point and starts to increase until reaching a value of 10^{20} cm^{-3}. Figure 3 shows that the efficiency increases when increase the doping density. This is because as the doping density of a solar cell increases, the series of resistance of the cell decreases. Conversely, when the doping density of a solar cell is increased, the series resistance is reduced, resulting in a considerable improvement in the fill factor [26].

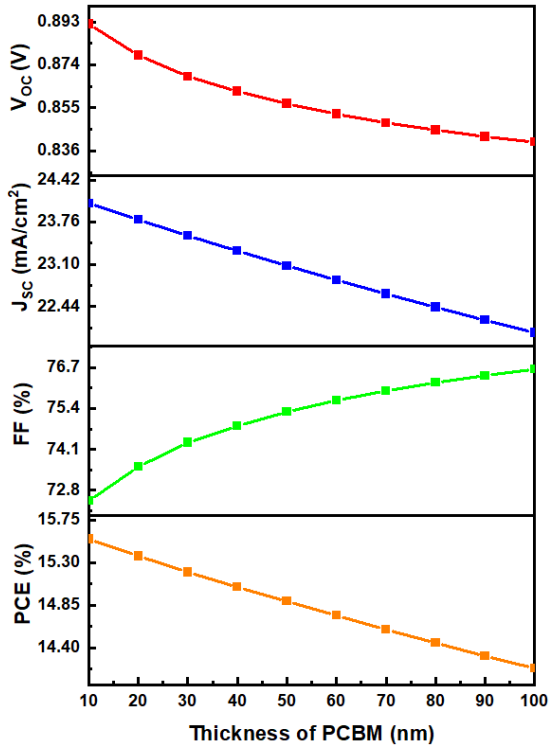

Fig. 2. The variation of PCBM thickness on PV parameters of simulated PSC

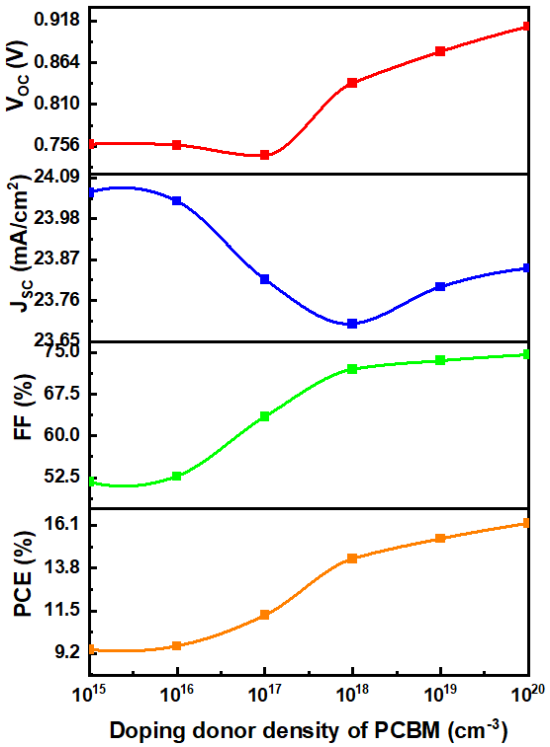

Fig. 3. The variation of PCBM doping donor density on PV parameters of simulated PSC

3.3 Effect of $MAPbI_3$ Thickness and Doping Acceptor Density

The absorber layer of PSC is made of perovskite. The layer is of significant importance in the context of its high light absorption capacity since it directly impacts the performance of perovskite solar cells (PSCs). In the field of PSCs, lead-based perovskites are commonly used as absorber layer. They are high-performance photovoltaic materials known for their wide bandgap, high absorption coefficient, low exciton binding energy, and high carrier mobility [27-30]. Moreover, the potential commercialization of perovskite solar cells (PSCs) is encouraging, primarily attributed to the

utilization of perovskite materials. This is mainly owing to their cost-effectiveness and diverse deposition processes, which enable the formation of superior-quality thin films throughout the manufacturing process. In order to get a high-power conversion efficiency (PSC), the perovskite layer is systematically optimized by considering two factors: the thickness and the doping acceptor density. The thickness of absorber layer is one of the crucial parameters in determining the performance of PSC. Initially, the thickness of absorber layer was varied in the range of 100 nm to 1000 nm, to observe the trend of the efficiency of PSC first. Next, further analysis was done to obtain the maximum efficiency of solar cells that can be achieved by an optimum thickness of absorber layer.

Figure 4 illustrates a notable increase in both V_{OC} and J_{SC} when the thickness of the perovskite layer is increased. Typically, a decrease in the thickness of the perovskite layer leads to a reduction in light absorption and the formation of excitons, hence impacting the J_{SC}. In instances when the thickness is substantial, a portion of the charge carriers undergo recombination prior to their departure from the surface [31]. The increase in perovskite thickness resulted in a rise in J_{SC}, which may be attributed to the enhanced absorption of photons with longer wavelengths inside the thicker perovskite layer. According to the results shown in Figure 4, the fill factor (FF) exhibited a decline from 76.02% to 73.33% when the thickness of the perovskite layer was increased.

Next, the obtained findings proved that the thickness of the perovskite layer did affect the efficiency of PSC. The power conversion efficiency (PCE) enhanced from 6.97% to 15.37% when the thickness of the perovskite layer was extended to 700 nm. However, the PCE showed only a marginal improvement beyond the 800 nm mark. The risk of charge recombination rises with increasing absorber layer thickness because a more extended diffusion means a greater distance travelled by the charge [23]. Inadequate light absorption likely causes less electron-hole pair production, leading to reduced PCE when the absorber layer is thinner [23]. Moreover, the rise in PCE is due to the charge carrier's diffusion length being larger than the absorber's thickness, resulting in most of the charge carriers getting to the electrode. Overmuch thickness, on the other hand, increases recombination because it creates a longer route for the charge carriers generated by photogeneration to travel [22]. The performance of the PSC is affected not only by the thickness of the perovskite layer, but also by the doping acceptor concentration in the perovskite layer. In this study, the value of doping acceptor density was varied from 1×10^{15} cm^{-3} to 1×10^{20} cm^{-3}.

Figure 5 demonstrates that as the acceptor density grows, the open-circuit voltage (V_{OC}) exhibits an upward trend while the short-circuit current (J_{SC}) experiences a decline. The reduction in conductivity of the PSC is attributed to the presence of a smaller depletion area, resulting in less carrier collection [31-33]. The graph also demonstrates that the open-circuit voltage (V_{OC}) is contingent upon the doping density, owing to the escalation of the saturation current with increasing doping density. Subsequently, the fill factor and power conversion efficiency (PCE) display a closely aligned trajectory, demonstrating a steady fall until reaching a value of 10^{20} cm^{-3}.

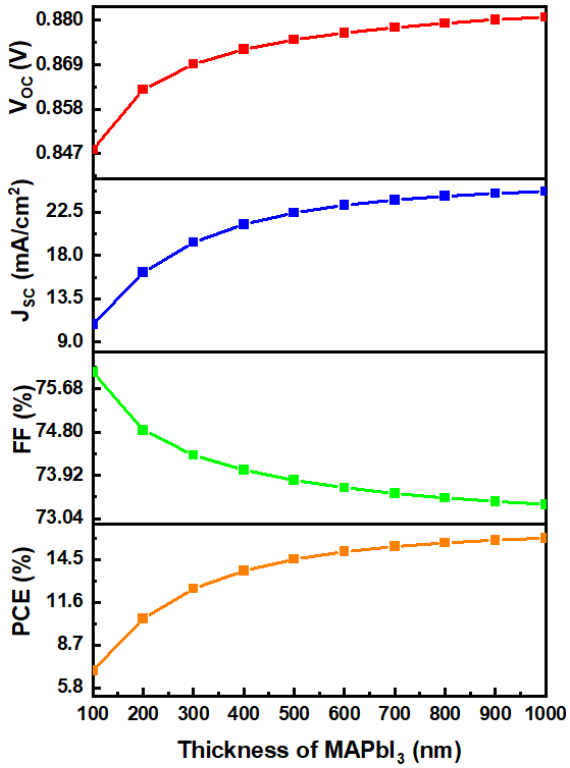

Fig. 4. The variation of MAPbI3 thickness on PV parameters of simulated PSC

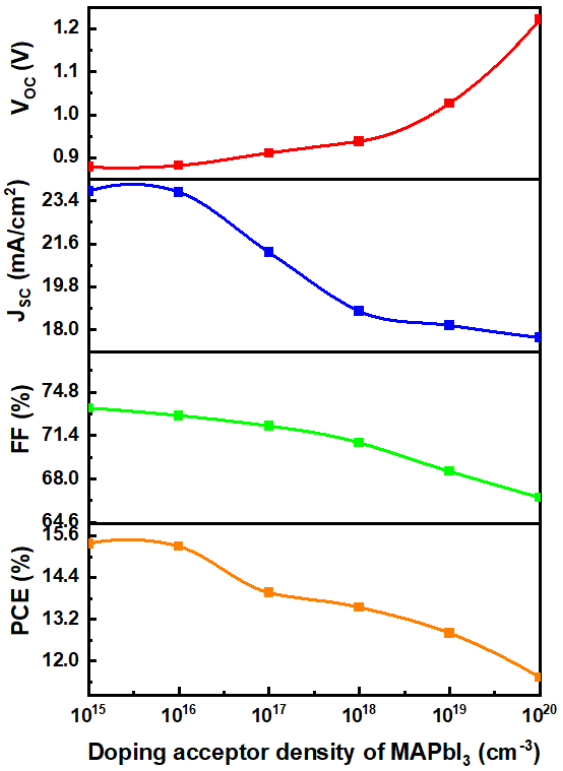

Fig. 5. The variation of $MAPbI_3$ doping acceptor density on PV parameters of simulated PSC

3.4 Effect of Doped PANI/GO Thickness and Doping Acceptor Density

The HTL is very crucial in PSC to enhance charge transportation and extraction [34,35]. A good HTL in high performance of solar cell should accept the holes from the light absorber efficiently, operate rapid transportation, and hole (HTL)-electron (ETL) recombination can be suppressed as much as possible. Furthermore, aligning the energy level of the hole transport material (HTM) with that of the absorber layer is essential. This alignment enhances the efficient transmission of holes and prevents the migration of photo-generated electrons towards the opposing electrodes [36]. To attain a high-power conversion efficiency (PSC), the optimization of the hole transport layer is conducted methodically, taking into account two key factors: the thickness of the layer and the density of the doping acceptors.

The effect of thickness is measured by varying the layer thickness of doped PANI/GO from a range of 100 nm to 1000 nm. The HTL facilitates the transport of holes from the absorber layer to the electrode, establishing a barrier that separates the absorber layer from the electrode. When the thickness of the hole transport layer (HTL) exceeds a certain threshold, the series resistance experiences an increase, hence impeding the efficient transportation of holes to the electrode [31].

On the other hand, in the event that the HTL has a thin structure, it may fail to provide an adequate amount of spacing between these layers. Recombination at the interface of the perovskite layer and electrode may occur as a consequence [31,20]. The Figure 6 shows that the photovoltaic characteristics remained unaltered. Only J_{SC} and fill factor increased slightly from 23.79648 mA/cm^2 to 23.79809 mA/cm^2 and 73.55% to 73.56%, respectively, as the thickness grew from 100 nm to 1000 nm. In general, the observed differences in the thickness of doped PANI/GO resulted in a marginal enhancement of the PCE, as seen in Figure 6.

Generally, doping density happens at the HTL where, both has density of acceptor, N_A. In this study, doping at HTL layer was varied with a range from 1×10^{15} cm^{-3} to 1×10^{20} cm^{-3}. Figure 7 illustrates that an increase in acceptor density leads to an increasing trend in the open-circuit voltage (V_{OC}), whereas the short-circuit current (J_{SC}) shows a decrease. The decrease in conductivity of the PSC may be explained by the existence of a diminished depletion region, leading to a reduced collection of carriers. Based on Figure 7, the highest efficiency of PSC obtained is at doping acceptor density of 1×10^{20} cm^{-3} while doping acceptor density that produced the lowest performance of PSC is 1×10^{15} cm^{-3}. Thus, it can be said that the efficiency of solar cells increases along with the increase of doping acceptor density of doped PANI/GO. This is because as HTL acceptor doping concentration increases, the resistivity of HTL is reduced. Hence, the current in a solar cell will be enhanced and caused the efficiency to increase. Thus, by increasing the doping acceptor density, the enhancement of the conductivity of the device will increase too. However, if the doping continues to increase to a certain extent, it will cause a Moss-Burstein effect due to heavy doping. This will eventually impede the performance of solar cells as an additional recombination center was created [23].

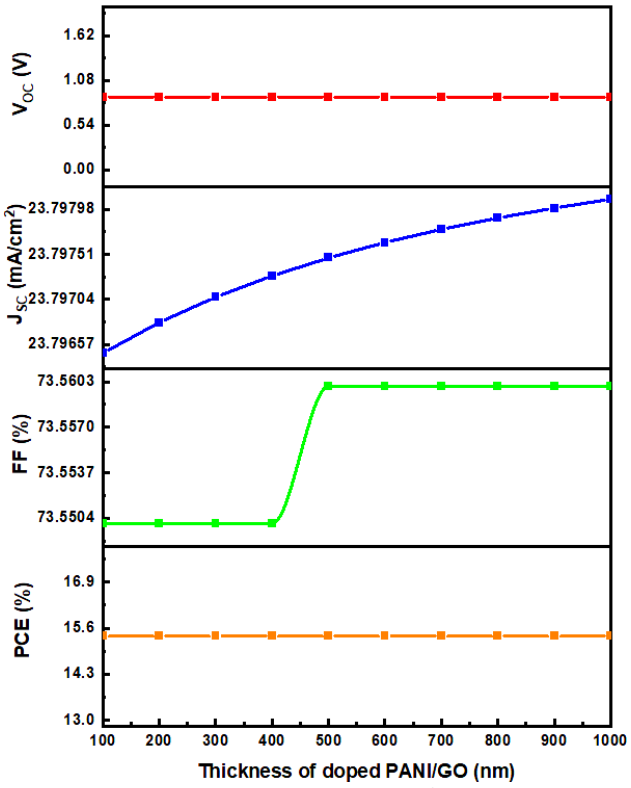

Fig. 6. The variation of doped PANI/GO thickness on PV parameters of simulated PSC

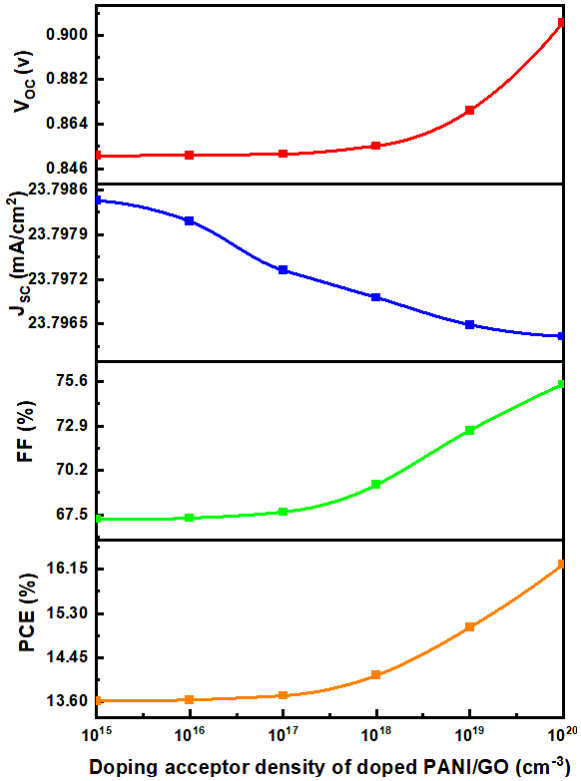

Fig. 7. The variation of doped PANI/GO doping density on PV parameters of simulated PSC

3.5 Optimized Device Performance

By simulating the solar cell structure in SCAPS-1D software, the optimized value for both parameters, thickness and doping density were obtained (Table 5). In the process of device manufacture, potential cost reduction benefits are associated with lowering the thickness of ETL, perovskite and HTL. Therefore, we chose a thickness of 20 nm for the electron transport layer (ETL), 700 nm for the perovskite layer and 100 nm for the hole transport layer (HTL) as the optimum value. A doping concentration of 1×10^{19} cm^{-3}, 1×10^{15} cm^{-3} and 2×10^{19} cm^{-3} were chosen for ETL, perovskite and HTL, respectively.

The J-V graph comparison is plotted in Figure 8. The photovoltaic device with an optimized structure of perovskite solar cells (PSCs) using doped PANI/GO as the hole transport layer (HTL) demonstrates a V_{OC} of 0.8782 V, a J_{SC} of 23.796476 mA/cm^2, a fill factor of 73.55%, and a PCE of 15.37%. This work presented an improved efficiency of 40% from the experimental data. The simulation findings demonstrate the importance of hole transport layers (HTLs) in facilitating charge extraction. Based on the findings of the optimized outcomes, it has been empirically shown that doped PANI/GO has promise as a viable hole transport layer (HTL) in perovskite solar cells (PSCs).

Table 5
Optimized device performance

Parameters	PCBM	$MAPbI_3$	Doped PANI/GO
Layer thickness, d (nm)	20	700	100
Doping density (cm^{-3})	1.0×10^{19}	1.0×10^{15}	2.0×10^{19}

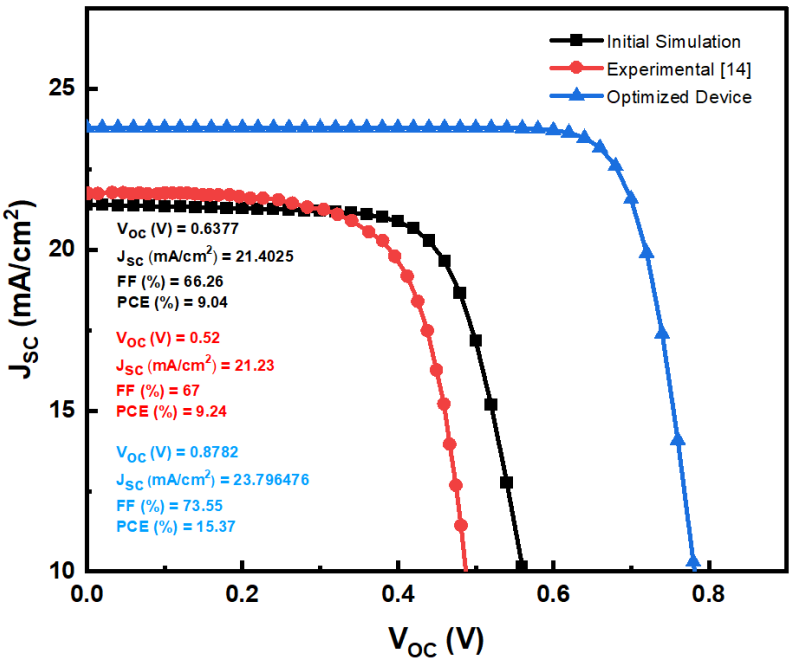

Fig. 8. J-V graph of PSC device for initial simulation, experimental and optimized device

4. Conclusions

This study provides a comparative analysis of experimental observations and SCAPS-1D simulations of perovskite solar cells using doped PANI/GO as HTL. The performance of PSCs is affected by many factors, including the thickness and doping densities of the ETL, perovskite and HTL layers. These parameters were thoroughly examined due to their substantial impact on the device's performance. After conducting optimizations, it was shown that the use of PSC with doped PANI/GO as the hole transport layer (HTL) resulted in the attainment of optimal performance. The achieved values were a V_{OC} of 0.8782 V, a J_{SC} of 23.796476 mA/cm^2, a fill factor of 73.55%, and a PCE of 15.37%. This work presented an improved efficiency of 40% from the experimental data. The findings demonstrated in this study can potentially be used in developing more affordable PSCs with improved performance.

Acknowledgement
The authors would like to thank the Ministry of Higher Education (MOHE) for sponsoring this work under project (FRGS/1/2022/TK07/UTEM/02/47) and MiNE, CeTRI, Faculty of Electronics & Computer Technology and Engineering (FTKEK), Universiti Teknikal Malaysia Melaka (UTeM) for the moral support throughout the project. The authors would also like to thank Dr. Marc Burgelman of the University of Gent in Belgium for supplying the SCAPS 1D simulation program.

References

[1] Novoselov, Kostya S., Andre K. Geim, Sergei Vladimirovich Morozov, Dingde Jiang, Michail I. Katsnelson, Irina V. Grigorieva, Sergey V. Dubonos, and Alexandr A. Firsov. "Two-dimensional gas of massless Dirac fermions in graphene." *nature* 438, no. 7065 (2005): 197-200. https://doi.org/10.1038/nature04233

[2] Mandal, Peetam, Jhuma Debbarma, and Mitali Saha. "A review on the emergence of graphene in photovoltaics industry." *Biointerface Research in Applied Chemistry* 11, no. 6 (2021): 15009-15036. https://doi.org/10.33263/BRIAC116.1500915036

[3] Lee, Changgu, Xiaoding Wei, Jeffrey W. Kysar, and James Hone. "Measurement of the elastic properties and intrinsic strength of monolayer graphene." *science* 321, no. 5887 (2008): 385-388. https://doi.org/10.1126/science.1157996

[4] Tiwari, Santosh K., Sumanta Sahoo, Nannan Wang, and Andrzej Huczko. "Graphene research and their outputs: Status and prospect." *Journal of Science: Advanced Materials and Devices* 5, no. 1 (2020): 10-29. https://doi.org/10.1016/j.jsamd.2020.01.006

[5] Ganz, Eric, Ariel B. Ganz, Li-Ming Yang, and Matthew Dornfeld. "The initial stages of melting of graphene between 4000 K and 6000 K." *Physical Chemistry Chemical Physics* 19, no. 5 (2017): 3756-3762. https://doi.org/10.1039/C6CP06940A

[6] Yu, Ting, Feng Wang, Yang Xu, Lingling Ma, Xiaodong Pi, and Deren Yang. "Graphene coupled with silicon quantum dots for high-performance bulk-silicon-based Schottky-junction photodetectors." *Advanced Materials* 28, no. 24 (2016): 4912-4919. https://doi.org/10.1002/adma.201506140

[7] Hashim, Norazlina, Rabiatul Manisah Mohamed, Hajaratul Najwa Mohamed, and Kamal Yusoh. "Poly (lactic acid)/graphene oxide nanocomposites: A morphology study and mechanism of reaction." *Journal of Advanced Research in Applied Sciences and Engineering Technology* 33, no. 3 (2023): 384-392. https://doi.org/10.37934/araset.33.3.384392

[8] Rashid, Nur Nadhirah Mohamad, Muhammad Quisar Lokman, Siti Nur Fatin Zuikafly, Nur Azmah Nordin, Hafizal Yahaya, Mohammad Faizal Ismail, Harith Ahmad, Wan Mohd Fazli Wan Nawawi, and Fauzan Ahmad. "Passively Q-switched erbium-doped fibre laser based on graphene-chitin saturable absorber." *Journal of Advanced Research in Applied Sciences and Engineering Technology* 33, no. 1 (2023): 44-52. https://doi.org/10.37934/araset.33.1.4452

[9] Wu, Zhongwei, Sai Bai, Jian Xiang, Zhongcheng Yuan, Yingguo Yang, Wei Cui, Xingyu Gao, Zhuang Liu, Yizheng Jin, and Baoquan Sun. "Efficient planar heterojunction perovskite solar cells employing graphene oxide as hole conductor." *Nanoscale* 6, no. 18 (2014): 10505-10510. https://doi.org/10.1039/C4NR03181D

[10] Palma, Alessandro L., Lucio Cinà, Sara Pescetelli, Antonio Agresti, Michele Raggio, Roberto Paolesse, Francesco Bonaccorso, and Aldo Di Carlo. "Reduced graphene oxide as efficient and stable hole transporting material in mesoscopic perovskite solar cells." *Nano Energy* 22 (2016): 349-360. https://doi.org/10.1016/j.nanoen.2016.02.027

[11] You, Peng, Zhike Liu, Qidong Tai, Shenghua Liu, and Feng Yan. "Efficient semitransparent perovskite solar cells with graphene electrodes." *Advanced Materials* 27, no. 24 (2015): 3632-3638. https://doi.org/10.1002/adma.201501145

[12] Kang, Aniseh Kafi, M. Hossein Zandi, and Nima E. Gorji. "Simulation analysis of graphene contacted perovskite solar cells using SCAPS-1D." *Optical and Quantum Electronics* 51 (2019): 1-9. https://doi.org/10.1007/s11082-019-1802-3

[13] Mabrouk, Sally, Ashim Gurung, Behzad Bahrami, Abiral Baniya, Raja Sekhar Bobba, Fan Wu, Rajesh Pathak, and Quinn Qiao. "Electrochemically prepared polyaniline as an alternative to poly (3, 4-ethylenedioxythiophene)-poly (styrenesulfonate) for inverted perovskite solar cells." *ACS Applied Energy Materials* 5, no. 8 (2022): 9351-9360. https://doi.org/10.1021/acsaem.2c00621

[14] Habib, M., M. Feteha, M. Soliman, A. Abdel Motagaly, S. El-Sheikh, and Sh Ebrahim. "Effect of doped polyaniline/graphene oxide ratio as a hole transport layer on the performance of perovskite solar cell." *Journal of Materials Science: Materials in Electronics* 31, no. 21 (2020): 18870-18882. https://doi.org/10.1007/s10854-020-04425-0

[15] Mabrouk, Sally, Behzad Bahrami, Hytham Elbohy, Khan Mamun Reza, Ashim Gurung, Mao Liang, Fan Wu, Mingtai Wang, Shangfeng Yang, and Qiquan Qiao. "Synergistic engineering of hole transport materials in perovskite solar cells." *InfoMat* 2, no. 5 (2020): 928-941. https://doi.org/10.1002/inf2.12062

[16] Kaharudin, Khairil Ezwan, and Fauziyah Salehuddin. "Predictive modeling of mixed halide perovskite cell using hybrid L27 OA Taguchi-based GA-MLR-GA approach." *Jurnal Teknologi* 84, no. 1 (2022): 1-9. https://doi.org/10.11113/jurnalteknologi.v84.15550

[17] Johari, Nur Aliesa, Nabilah Ahmad Jalaludin, Fauziyah Salehuddin, Faiz Arith, Khairil Ezwan Kaharudin, Anis Suhaila Mohd Zain, Siti Aisah Mat Junos, and Ibrahim Ahmad. "Analysis of inverted planar perovskite solar cells with graphene oxide as HTL using L9 OA Taguchi method." *Journal of Advanced Research in Micro and Nano Engineering* 16, no. 1 (2024): 48-60. https://doi.org/10.37934/armne.16.1.4860

[18] Ouslimane, Touria, Lhoussayne Et-Taya, Lahoucine Elmaimouni, and Abdellah Benami. "Impact of absorber layer thickness, defect density, and operating temperature on the performance of $MAPbI_3$ solar cells based on ZnO electron transporting material." *Heliyon* 7, no. 3 (2021). https://doi.org/10.1016/j.heliyon.2021.e06379

[19] Mandadapu, Usha, S. Victor Vedanayakam, and K. Thyagarajan. "Simulation and analysis of lead based perovskite solar cell using SCAPS-1D." *Indian Journal of Science and Technology* 10, no. 11 (2017): 65-72. https://doi.org/10.17485/ijst/2017/v10i11/110721

[20] Widianto, Eri, Erlyta Septa Rosa, Kuwat Triyana, Natalita Maulani Nursam, and Iman Santoso. "Performance analysis of carbon-based perovskite solar cells by graphene oxide as hole transport layer: Experimental and numerical simulation." *Optical materials* 121 (2021): 111584. https://doi.org/10.1016/j.optmat.2021.111584

[21] Gupta, Siddharth, Pratik Joshi, and Jagdish Narayan. "Electron mobility modulation in graphene oxide by controlling carbon melt lifetime." *Carbon* 170 (2020): 327-337. https://doi.org/10.1016/j.carbon.2020.07.073

[22] Hao, Liangsheng, Min Zhou, Yubao Song, Xinxia Ma, Jiang Wu, Qunzhi Zhu, Zaiguo Fu, Yihao Liu, Guoyu Hou, and Tong Li. "Tin-based perovskite solar cells: Further improve the performance of the electron transport layer-free structure by device simulation." *Solar Energy* 230 (2021): 345-354. https://doi.org/10.1016/j.solener.2021.09.091

[23] Anwar, Farhana, Rafee Mahbub, Sakin Sarwar Satter, and Saeed Mahmud Ullah. "Effect of different HTM layers and electrical parameters on ZnO nanorod-based lead-free perovskite solar cell for high-efficiency performance." *International Journal of Photoenergy* 2017, no. 1 (2017): 9846310. https://doi.org/10.1155/2017/9846310

[24] Abidin, Nurul Aliyah Zainal, Faiz Arith, Adri Aflah Shahrin Amri, Ahmad Nizamuddin Mustafa, Hafez Sarkawi, Mohd Shahadan Mohd Suan, Ahmad Syahiman Mohd Shah, Siti Aisah Junos, and Fauziyah Salehuddin. "Growth time dependence on ZnO nanorods photoanode for solar cell applications." *Journal of Advanced Research in Applied Sciences and Engineering Technology* 31, no. 2 (2023): 339-351. https://doi.org/10.37934/araset.31.2.339351

[25] Jeyakumar, R., Atanu Bag, Reza Nekovei, and R. Radhakrishnan. "Influence of electron transport layer (TiO_2) thickness and its doping density on the performance of $CH_3NH_3PbI_3$-based planar perovskite solar cells." *Journal of Electronic Materials* 49, no. 6 (2020): 3533-3539. https://doi.org/10.1007/s11664-020-08041-w

[26] Nithya, K. S., and K. S. Sudheer. "Device modelling of non-fullerene organic solar cell with inorganic CuI hole transport layer using SCAPS 1-D." *Optik* 217 (2020): 164790. https://doi.org/10.1016/j.ijleo.2020.164790

[27] Mahajan, Prerna, Ram Datt, Wing Chung Tsoi, Vinay Gupta, Amit Tomar, and Sandeep Arya. "Recent progress, fabrication challenges and stability issues of lead-free tin-based perovskite thin films in the field of photovoltaics." *Coordination Chemistry Reviews* 429 (2021): 213633. https://doi.org/10.1016/j.ccr.2020.213633

[28] Miyata, Atsuhiko, Anatolie Mitioglu, Paulina Plochocka, Oliver Portugall, Jacob Tse-Wei Wang, Samuel D. Stranks, Henry J. Snaith, and Robin J. Nicholas. "Direct measurement of the exciton binding energy and effective masses for charge carriers in organic–inorganic tri-halide perovskites." *Nature Physics* 11, no. 7 (2015): 582-587. https://doi.org/10.1038/nphys3357

[29] Huang, Jinsong, Yongbo Yuan, Yuchuan Shao, and Yanfa Yan. "Understanding the physical properties of hybrid perovskites for photovoltaic applications." *Nature Reviews Materials* 2, no. 7 (2017): 1-19. https://doi.org/10.1038/natrevmats.2017.42

[30] Jeon, Nam Joong, Hyejin Na, Eui Hyuk Jung, Tae-Youl Yang, Yong Guk Lee, Geunjin Kim, Hee-Won Shin, Sang Il Seok, Jaemin Lee, and Jangwon Seo. "A fluorene-terminated hole-transporting material for highly efficient and stable perovskite solar cells." *Nature Energy* 3, no. 8 (2018): 682-689. https://doi.org/10.1038/s41560-018-0200-6

[31] De Los Santos, I. Montoya, Hugo J. Cortina-Marrero, M. A. Ruíz-Sánchez, L. Hechavarría-Difur, F. J. Sánchez-Rodríguez, Maykel Courel, and Hailin Hu. "Optimization of CH3NH3PbI3 perovskite solar cells: A theoretical and experimental study." *Solar Energy* 199 (2020): 198-205. https://doi.org/10.1016/j.solener.2020.02.026

[32] Srivastava, Shristy, Anand Kumar Singh, Prashant Kumar, and Basudev Pradhan. "Comparative performance analysis of lead-free perovskites solar cells by numerical simulation." *Journal of Applied Physics* 131, no. 17 (2022). https://doi.org/10.1063/5.0088099

[33] Noorasid, Nur Syamimi, Faiz Arith, Ahmad Nizamuddin Mustafa, Puvaneswaran Chelvanathan, Mohammad Istiaque Hossain, Mohd Asyadi Azam, and Nowshad Amin. "Improved performance of lead-free Perovskite solar cell incorporated with TiO_2 ETL and CuI HTL using SCAPs." *Applied Physics A* 129, no. 2 (2023): 132. https://doi.org/10.1007/s00339-022-06356-5

[34] Noorasid, Nur Syamimi, Faiz Arith, Ain Yasmin Firhat, Ahmad Nizamuddin Mustafa, and Ahmad Syahiman Mohd Shah. "SCAPS numerical analysis of solid-state dye-sensitized solar cell utilizing copper (I) iodide as hole transport layer." *Engineering Journal* 26, no. 2 (2022): 1-10. https://doi.org/10.4186/ej.2022.26.2.1

[35] Aliyaselvam, Omsri Vinasha, Faiz Arith, Ahmad Nizamuddin Mustafa, Puvaneswaran Chelvanathan, Mohd Asyadi Azam, and Nowshad Amin. "Incorporation of green solvent for low thermal budget flower-like Copper (I) Iodide (γ-CuI) for high-efficiency solar cell." *Journal of Materials Science: Materials in Electronics* 34, no. 16 (2023): 1274. https://doi.org/10.1007/s10854-023-10578-5

[36] Vasilopoulou, Maria, Azhar Fakharuddin, Athanassios G. Coutsolelos, Polycarpos Falaras, Panagiotis Argitis, Abd Rashid bin Mohd Yusoff, and Mohammad Khaja Nazeeruddin. "Molecular materials as interfacial layers and additives in perovskite solar cells." *Chemical Society Reviews* 49, no. 13 (2020): 4496-4526. https://doi.org/10.1039/C9CS00733D